

Audio-Visual Contrastive Learning for Self-supervised Action Recognition

Haoyuan Lan, Yang Liu, and Liang Lin

Abstract—The underlying correlation between audio and visual modalities within videos can be utilized to learn supervised information for unlabeled videos. In this paper, we present an end-to-end self-supervised framework named Audio-Visual Contrastive Learning (AVCL), to learn discriminative audio-visual representations for action recognition. Specifically, we design an attention based multi-modal fusion module (AMFM) to fuse audio and visual modalities. To align heterogeneous audio-visual modalities, we construct a novel co-correlation guided representation alignment module (CGRA). To learn supervised information from unlabeled videos, we propose a novel self-supervised contrastive learning module (SelfCL). Furthermore, to expand the existing audio-visual action recognition datasets and better evaluate our framework AVCL, we build a new audio-visual action recognition dataset named Kinetics-Sounds100. Experimental results on Kinetics-Sounds32 and Kinetics-Sounds100 datasets demonstrate the superiority of our AVCL over the state-of-the-art methods on large-scale action recognition benchmark.

Index Terms—Action Recognition, Contrastive Learning, Audio-Visual

I. INTRODUCTION

WITH the development of deep learning, many visual recognition tasks have achieved state-of-the-art performance. This can be primarily attributed to the learned rich representation from well-trained networks using large-scale image/video datasets with strong supervision information [1]–[3]. For action recognition, both hand-crafted methods [4]–[8] and deep learning methods [9]–[13] require well-annotated large-scale datasets to train a robust model. However, annotating such large-scale data is laborious, expensive, and impractical, especially for data-driven high-level tasks like video action recognition. To fully leverage the large amount of unlabeled data, self-supervised learning gives a reasonable way to utilize unlabeled data to obtain supervision signals.

Self-supervised learning [14] generates supervision signals by adopting various pretext tasks or contrastive learning methods. The pretext task learning methods for the video data includes Odd-one-out [15], Sorting sequences [16], Order verification [17], Order prediction [18], and Temporal Contrastive Graph Learning [19], etc. Besides, many contrastive learning methods have been proposed, such as the NCE [20], MoCo [21], BYOL [22], SimCLR [23], SimSam [24], Barlow Twins [25]. However, the existing self-supervised learning methods

usually focus on single modality and ignore alignment and fusion of heterogeneous data from multiple modalities. Actually, the audio is another modality accompanied by the video [26], which contains complementary information that can improve the representation ability of video features [27]. To fully leverage the knowledge from audio, the audio-visual representation learning [28]–[31] has attracted increasing attention recently.

Actually, visual content and audio events tend to occur together. For a dynamic audio-visual video, the audio contains much complementary information of RGB image series, which can alleviate the problem that some video samples are indistinguishable in terms of appearance (e.g., playing the guitar and playing the violin). The advantages of audio modality has also been verified in video understanding [27]–[39], which can be classified into supervised learning and self-supervised learning, respectively. Though most of them are supervised methods, self-supervised learning provides the opportunity for exploiting large-scale unlabelled data. The audio-visual co-occurrences provide free supervised signals, which can be utilized for co-training a joint model and learning cross-modal representations. For instance, L3 [32] trained a audio-visual model to judge whether the image and audio clip are corresponding or not. AVE-Net [33] revised their previous model L3 to find the visual area with the maximum similarity for the current audio clip. CMA [36] proposed a co-attention based framework to learn generic cross-modal representations from unlabelled videos. However, previous approaches overlook the information exchange between modalities, and they are pervasively limited by the huge heterogeneous modality differences between audio and RGB image modalities.

In this paper, we focus on how to learn discriminative self-supervised audio-visual representations efficiently. Specifically, we consider audio as a primal modality to provide complementary information for visual modalities (RGB images) in action recognition and propose a novel contrastive learning algorithm framework named Audio-Visual Contrastive Learning (AVCL) to learn cross-modality features with strong representation ability. The AVCL is a self-supervised framework that integrates multi-modality alignment, multi-modal fusion and contrastive learning into an end-to-end manner. The main contributions of this paper are as follows:

- 1) To fully fuse complementary information between audio and visual modalities, we design a novel attention based multi-modal fusion module (AMFM).
- 2) Since there exists huge modality divergence between audio and visual data, we construct a novel co-correlation guided representation alignment module (CGRA) to align heterogeneous audio-visual data.

This work is supported in part by the National Natural Science Foundation of China under Grant No.62002395, and in part by the National Natural Science Foundation of Guangdong Province (China) under Grant No. 2021A15150123. (Corresponding author: Yang Liu)

H. Lan, Y. Liu, and L. Lin are with the School of Computer Science and Engineering, Sun Yat-sen University, Guangzhou, China. (e-mail: lanhy5@mail2.sysu.edu.cn; liuy856@mail.sysu.edu.cn; linliang@ieee.org.).

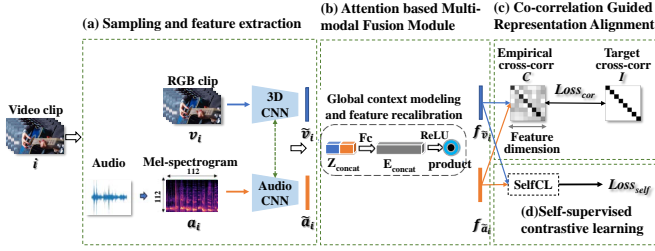


Fig. 1. The overall framework of the Audio-Visual Contrastive Learning (AVCL): (a) Sampling and Feature Extraction; (b) Attention based Multi-modal Fusion Module (AMFM); (c) Co-correlation Guided Representation Alignment (CGRA); (d) Self-supervised Contrastive Learning (SelfCL).

- 3) To learn discriminative unsupervised audio-visual representations for action recognition, we propose a novel self-supervised contrastive learning module (SelfCL).
- 4) We build a new audio-visual action recognition dataset named Kinetics-Sounds100 to expand the existing audio-visual datasets and better evaluate our framework.

II. METHODS

Given a video, the clips from this video are composed of frames with the size $c \times l \times h \times w$, where c is the number of channels, l is the number of frames, h and w indicate the height and width of frames. The size of the 3D convolutional kernel is $t \times d \times d$, where t is the temporal length and d is the spatial size. We define the sequence of video RGB tuples as $V = \langle v_1, v_2, \dots, v_i, \dots, v_N \rangle$, where v_i is an RGB image generated by continuously sampling m frames from a video O_i ($i = 1, \dots, N$). The audio mel-spectrogram tuples is represented as $A = \langle a_1, a_2, \dots, a_i, \dots, a_N \rangle$, where a_i is a mel-spectrogram generated from audio extracted from the video O_i , and \tilde{y}_i is the category label of the video O_i .

A. Sampling and Feature Extraction

RGB Processing: In this stage, we randomly sample consecutive frames from the video O_i ($i = 1, \dots, N$) to construct video RGB clip v_i . For RGB tuples, they contain dynamic information and strict temporal dependency of a video, which is essentially the global temporal structure of the videos.

Audio Processing: Different from the previous work which only extract 1.28s of audio, We extract the whole audio, and convert it to single-channel, and resample it to 24kHz. We then convert it to a mel-spectrogram representation using an STFT of window length 10ms, hop length 10ms and 256 frequency bands. This results in a 2D spectrogram a_i matrix of size 256×256 , after which we scale it by the mel-scale.

Feature Extraction: Although the audio modality has converted to a mel-spectrogram, it is still quite different from the RGB image due to the huge heterogeneous modality differences between the audio and RGB image representation. Therefore, using only one model to jointly learn the audio-visual is not feasible. To address this issue, we use two independent models with the same basic framework to extract the features for these two modalities, respectively. The parameters between these two models are not shared. The extracted feature for RGB clip v_i is denoted as \tilde{v}_i , the corresponding feature for audio mel-spectrogram a_i is denoted as \tilde{a}_i .

B. Attention based Multi-modal Fusion Module

To better fuse audio and visual modalities, we propose an Attention based Multi-modal Fusion Module (AMFM). Since the features from different modalities are correlated, we construct a cross-modal feature fusion module that receives features from different modalities and learns a global context embedding, then this embedding is used to recalibrate the input features from different modalities.

To utilize the correlation between these two modalities, we concatenate these two feature vectors and get joint representations through a fully-connected layer:

$$Z_u = W_s [\tilde{v}_i, \tilde{a}_i] + b_s \quad (1)$$

where $[\cdot, \cdot]$ denotes the concatenation operation, $Z_u \in \mathbb{R}^{c_u}$ denotes the joint representation, W_s and b_s are weights and bias of the fully-connected layer. To make use of the global context information aggregated in the joint representations Z_u , we predict excitation signal for it via a fully-connected layer:

$$E = W_e Z_u + b_e \quad (2)$$

where W_e and b_e are weights and biases of the fully-connected layer. After obtaining the excitation signal $E \in \mathbb{R}^c$, we use it to recalibrate the input feature \tilde{v}_i and \tilde{a}_i adaptively by a simple gating mechanism:

$$f_{\tilde{v}_i} = \sigma(E) \odot \tilde{v}_i \quad (3)$$

$$f_{\tilde{a}_i} = \sigma(E) \odot \tilde{a}_i \quad (4)$$

where \odot is channel-wise product operation for each element in the channel dimension, and $\sigma(\cdot)$ is the ReLU function. W_c and b_c are weights and biases of the fully-connected layer. In this way, we can allow the features of one modality to recalibrate the features of another modality while concurrently preserving the correlation among different modalities.

C. Co-correlation Guided Representation Alignment

Inspired by the cross-correlation matrix [25] that learns supervisory signal within one modality, we introduce a novel Co-correlation Guided Representation Alignment module (CGRA) to align heterogeneous audio-visual multi-modality data, The CGRA aims to strengthen the correlation between two modalities by making the cross-correlation matrix between the network outputs as close to the identity matrix as possible.

$$Loss_{cor} \triangleq \sum_i (1 - C_{ii})^2 + \lambda \sum_i \sum_{j \neq i} C_{ij}^2 \quad (5)$$

where λ is a positive constant trading off the importance of the first and second terms of the loss, and where C is the cross-correlation matrix computed between the outputs of the two identical networks along the batch dimension:

$$C_{ij} \triangleq \frac{\sum_b f_{\tilde{v}_i^b} f_{\tilde{a}_j^b}}{\sqrt{\sum_b (f_{\tilde{v}_i^b})^2} \sqrt{\sum_b (f_{\tilde{a}_j^b})^2}} \quad (6)$$

where b denotes batch samples. C is a square matrix with the same size as the network's output, and with values between -1 (perfect anti-correlation) and 1 (perfect correlation).

D. Self-supervised Contrastive Learning

The core of self-supervised contrastive learning is to make the distance between features from the same sample as close as possible, and the features from different samples as far away as possible. In this paper, we take the RGB clip feature v_i of the video O_i and the mel-spectrogram a_i generated by the corresponding audio as examples to clarify our self-supervised contrastive learning module (SelfCL).

In RGB modality, the contrastive loss is defined as:

$$\begin{aligned} Loss_v^{self} &= \sum_{i \in I} Loss_{f_{v_i}}^{self} \\ &= - \sum_{i \in I} \log \frac{h_{\theta}(f_{\tilde{v}_i} \cdot f_{\tilde{a}_i})}{\sum_{j \in I} h_{\theta}(f_{\tilde{v}_i} \cdot f_{\tilde{a}_j}) + \sum_{j \in A(i)} h_{\theta}(f_{\tilde{v}_i} \cdot f_{\tilde{v}_j})} \end{aligned} \quad (7)$$

Here, $i \in I \equiv \{1, \dots, N\}$, $A(i) \equiv I \setminus \{i\}$, $\tau \in R^+$ is a scalar temperature parameter. h_{θ} is the distance between two features, which is obtained by using the feature representation of non-parametric softmax:

$$h_{\theta}(f_{\tilde{v}_i} \cdot f_{\tilde{a}_j}) = \exp\left(\frac{f_{\tilde{v}_i} \cdot f_{\tilde{a}_j}}{\|f_{\tilde{v}_i}\| \cdot \|f_{\tilde{a}_j}\|} \cdot \frac{1}{\tau}\right) \quad (8)$$

Similarly, the contrastive loss for audio modality can be computed as:

$$\begin{aligned} Loss_a^{self} &= \sum_{i \in I} Loss_{f_{a_i}}^{self} \\ &= - \sum_{i \in I} \log \frac{h_{\theta}(f_{\tilde{a}_i} \cdot f_{\tilde{v}_i})}{\sum_{j \in I} h_{\theta}(f_{\tilde{a}_i} \cdot f_{\tilde{v}_j}) + \sum_{j \in A(i)} h_{\theta}(f_{\tilde{a}_i} \cdot f_{\tilde{a}_j})} \end{aligned} \quad (9)$$

Then, the overall contrastive loss is defined as follows:

$$Loss_{self} = Loss_v^{self} + Loss_a^{self} \quad (10)$$

The overall loss for our Audio-Visual Contrastive Learning (AVCL) framework is obtained by combing Eq. (5) and Eq. (10), where λ_{cor} and λ_{self} control the contribution of $Loss_{cor}$ and $Loss_{self}$, respectively:

$$Loss = \lambda_{cor} Loss_{cor} + \lambda_{self} Loss_{self} \quad (11)$$

III. EXPERIMENTS

We conduct experiments on two video datasets, namely, Kinetics-Sounds32 [32] and Kinetics-Sounds100.

A. Datasets

Kinetics-Sounds32 (K32). This dataset contains 19.2k videos (16.1k training, 1.1k validation, 2.0k test) from the Kinetics dataset with 34 action classes, which have been chosen to be potentially manifested visually and aurally.

Kinetics-Sounds100 (K100). To expand the existing audio-visual action recognition datasets and better evaluate our algorithm, we build a new audio-visual action recognition dataset named Kinetics-Sounds100. We take a subset from the Kinetics400 dataset [40], which contains YouTube videos manually annotated for human actions using Mechanical Turk, and cropped to 10 seconds around the action. The subset contains 61.3k videos (50.2k training, 3.9k validation, 7.2k

TABLE I
ACTION RECOGNITION ACCURACY (%) WITH DIFFERENT SAMPLING METHODS AND DIFFERENT NUMBER OF MODELS ON K32.

RGB length	Audio length	Model number	Accuracy
16	Raw audio	2	50.2
1	1.2s Mel-spectrogram	2	67.9
16	Whole Mel-spectrogram	2	75.6
16	Whole Mel-spectrogram	1	60.5

testing) from the Kinetics400 dataset with 100 action classes. Including all the categories from K32, we supplement some challenging categories with similar appearance but different audio features. For example, dance (dancing charleston and belly dancing), sports (playing volleyball and playing cricket), and jubilation (applauding and celebrating), etc., increase the generalizability of the model.

B. Experimental Setting

Network Architecture. For video encoder, C3D [41], R3D [42] and R(2+1)D [43] are used as backbones, where the kernel size of 3D convolutional layers is set to $3 \times 3 \times 3$. The R3D network is implemented with no repetitions in conv2-5, which results in 9 convolution layers totally. The C3D network is modified by replacing the two fully connected layers with global spatiotemporal pooling layers. The R(2+1)D network has the same architecture as the R3D with only 3D kernels decomposed. Dropout layers are applied between fully-connected layers with $p = 0.7$. The feature extraction network output of the pre-training process is 512 channels.

Parameters. Following the settings in [18], [44], we set the clip length of input video as 16. RGB images and mel-spectrograms are randomly cropped to 112×112 . Two independent models with the same backbone are utilized for two modalities, respectively. We set the parameters $\lambda = 0.005$ for $Loss_{cor}$, and $\lambda_{cor} = 0.9$, $\lambda_{self} = 0.1$ to balance the contribution between CGRA module and SelfCL module. To optimize the model, we use mini-batch SGD with the batchsize 16, the initial learning rate 0.001, the momentum 0.9 and the weight decay 0.0005 in training process, while the weight decay is set to 0.005 in finetune and test process. The training process lasts for 300 epochs, while the finetune and test lasts for 150 epochs. The model with the best validation accuracy is saved to the best model. Our method is implemented by PyTorch 1.3.0 with eight NVIDIA RTX 3090 GPUs.

C. Ablation Study

In this section, we conduct ablation studies with R3D as the backbone, to analyze the contribution of each component of our AVCL and some important hyperparameters. The evaluation metrics is the action recognition accuracy on K32 dataset.

The sampling methods of audio-visual features. To verify the effectiveness of our proposed sampling method, we compare our method with other sampling methods. It can be observed in Table I that our sampling method performs better than other methods. This verifies that the whole audio contains more comprehensive information and the RGB clip contains dynamic information and strict temporal dependency.

TABLE II
ACTION RECOGNITION ACCURACY (%) WITHOUT OR WITH DIFFERENT LAYER OF CO-CORRELATION GUIDED REPRESENTATION ALIGNMENT MODULE ON K32.

Backbone	CGRA	Layer	Accuracy
R3D	✗	None	72.5
R3D	✓	conv3	68.5
R3D	✓	conv4	69.3
R3D	✓	conv5	70.9
R3D	✓	pool-final	75.6
R3D	✓	conv5+pool	70.4

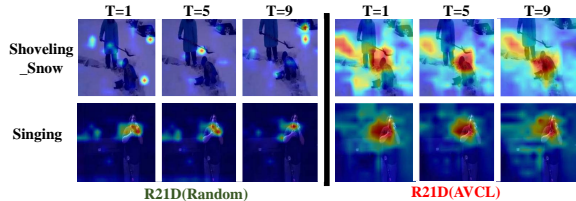


Fig. 2. Visualization of a sequence of activation maps on Kinetics-sounds dataset with R(2+1)D as the backbone.

The number of models. From Table I, we can see that two separated models can better model heterogeneous modalities and achieve better performance than that of using one model.

The CGRA module. To analyze the contribution of the CGRA module, we remove this module and apply it in different layer. It can be observed in Table II that our AVCL performs better than the AVCL without the CGRA. When the CGRA module is applied in the pool-final layer, the accuracy is the best. This verifies that the CGRA module can effectively align the high-level features of the two modalities.

The SelfCL module. To analyze the contribution of the SelfCL module, we remove this module and show its performance. To analyze the contribution of CGRA and SelfCL, we set different values to λ_{cor} and λ_{self} in Eq. (11), as shown in Table III. When setting the weight values of λ_{cor} and λ_{self} to 0.9 and 0.1, the accuracy is the best. These results validate that SelfCL, CGRA, and AMFM all contribute to the overall framework, while SelfCL contributes more than the CGRA due to the unavailable supervised information.

The AMFM module. To analyze the contribution of the AMFM, we remove this module and merely feed the concatenated features. It can be observed in Table III that our AVCL performs better than the AVCL without the AMFM. This verifies that the AMFM module can effectively fuse audio-visual modalities and learn discriminative representations.

D. Action Recognition

Our action recognition results are shown in Table IV, compared with six state-of-the-art methods, i.e., IIC [45], MoCo [21], BYOL [22], SimCLR [23], SimSam [24] and Barlow Twins [25]. **Baseline** is a supervised algorithm to extract features of different modalities through only one R3D network. To facilitate fair comparison with our method, we unify the inputs and outputs as RGB images and audio. Additionally, all comparison methods utilize two models without sharing parameters. Except for our AVCL, all comparison methods merely feed the concatenated features to compute the accuracy.

From Table IV, we can have the following observations: (1) With the same evaluation metric, our AVCL performs

TABLE III
ACTION RECOGNITION ACCURACY (%) WITH/WITHOUT SELF-SUPERVISED CONTRASTIVE LEARNING MODULE AND WITH DIFFERENT VALUES OF λ_{cor} AND λ_{self} , AS WELL AS WITH/WITHOUT ATTENTION BASED MULTI-MODAL FUSION MODULE ON K32.

Backbone	SelfCL	λ_{cor}	λ_{self}	AMFM	Accuracy
R3D	✗	1	0	✓	73.5
R3D	✓	0.1	0.9	✓	72.0
R3D	✓	0.3	0.7	✓	72.2
R3D	✓	0.5	0.5	✓	74.1
R3D	✓	0.7	0.3	✓	73.7
R3D	✓	0.9	0.1	✓	75.6
R3D	✓	0.9	0.1	✗	73.5

TABLE IV
COMPARISON WITH THE STATE-OF-THE-ART SELF-SUPERVISED CONTRASTIVE LEARNING METHODS ON K32 AND K100.

Method	Pretrain	Test	Backbone	K32	K100
Baseline-R	RGB	RGB	R3D	60.4	53.6
Baseline-A	Audio	Audio	R3D	52.9	40.9
Baseline-R+A	RGB+Audio	RGB+Audio	R3D	73.9	61.3
IIC [45]	RGB+Audio	RGB+Audio	R3D	60.5	46.4
SimCLR [23]	RGB+Audio	RGB+Audio	R3D	69.7	59.1
MoCo [21]	RGB+Audio	RGB+Audio	R3D	68.2	58.2
BYOL [22]	RGB+Audio	RGB+Audio	R3D	73.3	61.4
SimSam [24]	RGB+Audio	RGB+Audio	R3D	72.9	60.8
Barlow Twins [25]	RGB+Audio	RGB+Audio	R3D	69.6	59.3
AVCL(Ours)	RGB+Audio	RGB+Audio	R3D	75.6	64.4
AVCL(Ours)	RGB+Audio	RGB+Audio	C3D	74.0	61.3
AVCL(Ours)	RGB+Audio	RGB+Audio	R(2+1)D	77.2	67.1

favorably against existing approaches under the R3D backbone on both K32 and K100 datasets. (2) Compared with baseline in different modalities, our AVCL achieves significant improvement on both K32 and K100 datasets, which demonstrates the great potential of our AVCL in self-supervised video representation learning and the necessity of using audio modality. (3) After pre-trained with the R3D/C3D/R(2+1)D backbones, we outperform the current contrastive learning methods on both K32 and K100 datasets. This validates the scalability and effectiveness of the AVCL on different datasets.

E. Visualization Analysis

To have an intuitive understanding of the proposed AVCL, we visualize the spatiotemporal regions according to the class activation map, as shown in the Fig. 2. These examples demonstrate strong correlations between highly activated regions and dominant motions in the scene, which validates that our AVCL can effectively capture dominant motions in videos by learning discriminative audio-visual representations of videos.

IV. CONCLUSION

In this paper, we propose a novel framework for cross-modal action recognition based on audio-visual contrastive learning. We first describe attention based multi-modal fusion module and co-correlation guided representation alignment module, and then introduce a self-supervised contrastive learning which suitable for two modalities. Extensive experiments have been conducted on both Kinetics-Sounds32 dataset and the expanded Kinetics-Sounds100 dataset. Our method outperforms the state-of-the-art methods and also achieves favorable results in cross-modality scenarios.

REFERENCES

- [1] B. Schölkopf, F. Locatello, S. Bauer, N. R. Ke, N. Kalchbrenner, A. Goyal, and Y. Bengio, “Toward causal representation learning,” *Proc. IEEE*, vol. 109, no. 5, pp. 612–634, 2021.
- [2] K. Yu, X. Guo, L. Liu, J. Li, H. Wang, Z. Ling, and X. Wu, “Causality-based feature selection: Methods and evaluations,” *ACM Comput. Surv.*, vol. 53, no. 5, pp. 1–36, 2020.
- [3] Y. Liu, Y. Wei, H. Yan, G. Li, and L. Lin, “Causal reasoning with spatial-temporal representation learning: A prospective study,” *arXiv:2204.12037*, 2022.
- [4] I. Laptev, M. Marszalek, C. Schmid, and B. Rozenfeld, “Learning realistic human actions from movies,” in *Proc. IEEE Conf. Comput. Vis. Pattern Recognit.*, Anchorage, Alaska, USA, Jun. 2008, pp. 1–8.
- [5] H. Wang, A. Kläser, C. Schmid, and C.-L. Liu, “Dense trajectories and motion boundary descriptors for action recognition,” *Int. J. Comput. Vis.*, vol. 103, no. 1, pp. 60–79, 2013.
- [6] H. Wang and C. Schmid, “Action recognition with improved trajectories,” in *Proc. IEEE Int. Conf. Comput. Vis.*, Sydney, Australia, Dec. 2013, pp. 3551–3558.
- [7] Y. Liu, Z. Lu, J. Li, T. Yang, and C. Yao, “Global temporal representation based cnns for infrared action recognition,” *IEEE Signal Process. Lett.*, vol. 25, no. 6, pp. 848–852, 2018.
- [8] Y. Liu, Z. Lu, J. Li, and T. Yang, “Hierarchically learned view-invariant representations for cross-view action recognition,” *IEEE Trans. Circ. and Syst. Video Tech.*, vol. 29, no. 8, pp. 2416–2430, 2019.
- [9] R. Christoph and F. A. Pinz, “Spatiotemporal residual networks for video action recognition,” in *Proc. Neural Inf. Process. Syst.*, Barcelona, Spain, Dec. 2016, pp. 3468–3476.
- [10] C. Feichtenhofer, A. Pinz, and A. Zisserman, “Convolutional two-stream network fusion for video action recognition,” in *Proc. IEEE Conf. Comput. Vis. Pattern Recognit.*, NV, USA, Jun. 2016, pp. 1933–1941.
- [11] K. Simonyan and A. Zisserman, “Two-stream convolutional networks for action recognition in videos,” in *Proc. Neural Inf. Process. Syst.*, Montreal, Quebec, Canada, Dec. 2014, pp. 568–576.
- [12] Y. Liu, Z. Lu, J. Li, T. Yang, and C. Yao, “Deep image-to-video adaptation and fusion networks for action recognition,” *IEEE Trans. Image Process.*, vol. 29, pp. 3168–3182, 2020.
- [13] Y. Liu, K. Wang, G. Li, and L. Lin, “Semantics-aware adaptive knowledge distillation for sensor-to-vision action recognition,” *IEEE Trans. Image Process.*, vol. 30, pp. 5573–5588, 2021.
- [14] M. Liu, S. Wang, Y. Guo, Y. He, and H. Xue, “Pano-sfmlearner: Self-supervised multi-task learning of depth and semantics in panoramic videos,” *IEEE Signal Process. Lett.*, vol. 28, pp. 832–836, 2021.
- [15] B. Fernando, H. Bilen, E. Gavves, and S. Gould, “Self-supervised video representation learning with odd-one-out networks,” in *Proc. IEEE Conf. Comput. Vis. Pattern Recognit.*, Honolulu, HI, USA, Jul. 2017, pp. 3636–3645.
- [16] H.-Y. Lee, J.-B. Huang, M. Singh, and M.-H. Yang, “Unsupervised representation learning by sorting sequences,” in *Proc. IEEE Int. Conf. Comput. Vis.*, Venice, Italy, Oct. 2017, pp. 667–676.
- [17] I. Misra, C. L. Zitnick, and M. Hebert, “Shuffle and learn: unsupervised learning using temporal order verification,” in *Proc. IEEE Int. Conf. Comput. Vis.*, Amsterdam, The Netherlands, Oct. 2016, pp. 527–544.
- [18] D. Xu, J. Xiao, Z. Zhao, J. Shao, D. Xie, and Y. Zhuang, “Self-supervised spatiotemporal learning via video clip order prediction,” in *Proc. IEEE Conf. Comput. Vis. Pattern Recognit.*, Long Beach, CA, USA, Jun. 2019, pp. 10334–10343.
- [19] Y. Liu, K. Wang, L. Liu, H. Lan, and L. Lin, “Tcgl: Temporal contrastive graph for self-supervised video representation learning,” *IEEE Trans. Image Process.*, vol. 31, pp. 1978–1993, 2022.
- [20] M. Gutmann and A. Hyvärinen, “Noise-contrastive estimation: A new estimation principle for unnormalized statistical models,” in *Proc. 13th Int. Conf. Artif. Intell. Statist.*, Sardinia, Italy, May. 2010, pp. 297–304.
- [21] K. He, H. Fan, Y. Wu, S. Xie, and R. Girshick, “Momentum contrast for unsupervised visual representation learning,” in *Proc. IEEE Conf. Comput. Vis. Pattern Recognit.*, Seattle, WA, USA, Jun. 2020, pp. 9729–9738.
- [22] J.-B. Grill, F. Strub, F. Altché, C. Tallec, P. Richemond, E. Buchatskaya, C. Doersch, B. Avila Pires, Z. Guo, M. Gheshlaghi Azar *et al.*, “Bootstrap your own latent—a new approach to self-supervised learning,” in *Proc. Neural Inf. Process. Syst.*, Dec. 2020, pp. 21271–21284.
- [23] T. Chen, S. Kornblith, M. Norouzi, and G. Hinton, “A simple framework for contrastive learning of visual representations,” in *Proc. 37th Int. Conf. Mach. Learn.*, Jul. 2020, pp. 1597–1607.
- [24] X. Chen and K. He, “Exploring simple siamese representation learning,” in *Proc. IEEE Conf. Comput. Vis. Pattern Recognit.*, Jun. 2021, pp. 15750–15758.
- [25] J. Zbontar, L. Jing, I. Misra, Y. LeCun, and S. Deny, “Barlow twins: Self-supervised learning via redundancy reduction,” in *Proc. 38th Int. Conf. Mach. Learn.*, Jul. 2021, pp. 12310–12320.
- [26] M. Tagliasacchi, B. Gfeller, F. de Chaumont Quitry, and D. Roblek, “Pre-training audio representations with self-supervision,” *IEEE Signal Process. Lett.*, vol. 27, pp. 600–604, 2020.
- [27] E. Kazakos, A. Nagrani, A. Zisserman, and D. Damen, “Epic-fusion: Audio-visual temporal binding for egocentric action recognition,” in *Proc. IEEE Int. Conf. Comput. Vis.*, Seoul, Korea (South), Oct. 2019, pp. 5492–5501.
- [28] R. Gao, T.-H. Oh, K. Grauman, and L. Torresani, “Listen to look: Action recognition by previewing audio,” in *Proc. IEEE Conf. Comput. Vis. Pattern Recognit.*, Seattle, WA, USA, Jun. 2020, pp. 10457–10467.
- [29] P. Morgado, N. Vasconcelos, and I. Misra, “Audio-visual instance discrimination with cross-modal agreement,” in *Proc. IEEE Conf. Comput. Vis. Pattern Recognit.*, Jun. 2021, pp. 12475–12486.
- [30] H. Alwassel, D. Mahajan, B. Korbar, L. Torresani, B. Ghanem, and D. Tran, “Self-supervised learning by cross-modal audio-video clustering,” in *Proc. Neural Inf. Process. Syst.*, Dec. 2020, pp. 9758–9770.
- [31] H. Akbari, L. Yuan, R. Qian, W.-H. Chuang, S.-F. Chang, Y. Cui, and B. Gong, “Vatt: Transformers for multimodal self-supervised learning from raw video, audio and text,” *Advances in Neural Inf. Process. Syst.*, vol. 34, 2021.
- [32] R. Arandjelovic and A. Zisserman, “Look, listen and learn,” in *Proc. IEEE Int. Conf. Comput. Vis.*, Venice, Italy, Oct. 2017, pp. 609–617.
- [33] —, “Objects that sound,” in *Proceedings of the European conference on computer vision (ECCV)*, 2018, pp. 435–451.
- [34] Y. Aytar, C. Vondrick, and A. Torralba, “Soundnet: Learning sound representations from unlabeled video,” in *Proc. Neural Inf. Process. Syst.*, Barcelona, Spain, Dec. 2016, pp. 892–900.
- [35] A. Owens and A. A. Efros, “Audio-visual scene analysis with self-supervised multisensory features,” in *Proc. Eur. Conf. Comput. Vis.*, Munich, Germany, Sept. 2018, pp. 631–648.
- [36] Y. Cheng, R. Wang, Z. Pan, R. Feng, and Y. Zhang, “Look, listen, and attend: Co-attention network for self-supervised audio-visual representation learning,” in *Proc. ACM Int. Conf. Multimedia*, Seattle, WA, USA, Oct. 2020, pp. 3884–3892.
- [37] P. Morgado, Y. Li, and N. Vasconcelos, “Learning representations from audio-visual spatial alignment,” in *Proc. Neural Inf. Process. Syst.*, Dec. 2020, pp. 4733–4744.
- [38] B. Korbar, D. Tran, and L. Torresani, “Cooperative learning of audio and video models from self-supervised synchronization,” in *Proc. Neural Inf. Process. Syst.*, Dec. 2018, pp. 7774–7785.
- [39] J. Ngiam, A. Khosla, M. Kim, J. Nam, H. Lee, and A. Y. Ng, “Multimodal deep learning,” in *Proc. 28th Int. Conf. Mach. Learn.*, Bellevue, Washington, USA, Jun. 2011, pp. 689–696.
- [40] W. Kay, J. Carreira, K. Simonyan, B. Zhang, C. Hillier, S. Vijayanarasimhan, F. Viola, T. Green, T. Back, P. Natsev *et al.*, “The kinetics human action video dataset,” *arXiv:1705.06950*, 2017.
- [41] D. Tran, L. Bourdev, R. Fergus, L. Torresani, and M. Paluri, “Learning spatiotemporal features with 3d convolutional networks,” in *Proc. IEEE Int. Conf. Comput. Vis.*, Santiago, Chile, Dec. 2015, pp. 4489–4497.
- [42] H. Xu, A. Das, and K. Saenko, “R-c3d: Region convolutional 3d network for temporal activity detection,” in *Proc. IEEE Int. Conf. Comput. Vis.*, Venice, Italy, Oct. 2017, pp. 5783–5792.
- [43] D. Tran, H. Wang, L. Torresani, J. Ray, Y. LeCun, and M. Paluri, “A closer look at spatiotemporal convolutions for action recognition,” in *Proc. IEEE Conf. Comput. Vis. Pattern Recognit.*, Salt Lake City, UT, USA, Jun. 2018, pp. 6450–6459.
- [44] Y. Yao, C. Liu, D. Luo, Y. Zhou, and Q. Ye, “Video playback rate perception for self-supervised spatio-temporal representation learning,” in *Proc. IEEE Conf. Comput. Vis. Pattern Recognit.*, Seattle, WA, USA, Jun. 2020, pp. 6548–6557.
- [45] L. Tao, X. Wang, and T. Yamasaki, “Self-supervised video representation learning using inter-intra contrastive framework,” in *Proc. ACM Int. Conf. Multimedia*, Seattle, WA, USA, Oct. 2020, pp. 2193–2201.